Robust Method to Determine Critical Micelle Concentration via Spreading Oil Drops on Surfactant Solutions

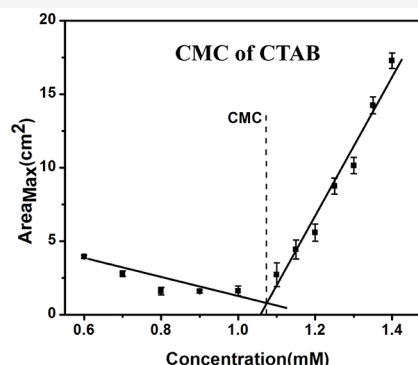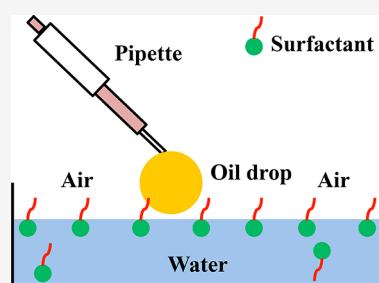Swaraj Deodhar, Pankaj Rohilla, M Manivannan, Sumesh P. Thampi,* and Madivala G. Basavaraj*

ACCESS | Metrics & More | Article Recommendations

ABSTRACT: The spreading of a liquid on another is often encountered in oil spills and coatings and is also of industrial relevance in pharmaceuticals and petrochemicals. In this study, the spreading of oil drops on aqueous solutions containing cationic, anionic, and nonionic surfactants over a wide range of surfactant concentrations is investigated. The spreading behavior quantified by measuring the time evolution of the projected area of the oil lens reveals the occurrence of a maximum, which is strongly dependent on the concentration of the surfactant in the aqueous solution. Our experiments show that this dependence is different at concentrations above and below the critical micelle concentration (CMC) of the surfactant and can be captured by two straight lines of different slopes. Interestingly, these two straight lines intersect at a concentration that coincides with the CMC of the surfactants in solution. We find that this behavior is universal as shown by performing experiments with different types of surfactants, their purity, and other system variables. Thus, we propose a method to unambiguously determine the CMC of surfactant solutions compared to the conventional techniques. The proposed method is simple, versatile, and applicable for the determination of CMC of both ionic and nonionic surfactants.

INTRODUCTION

Surfactant molecules are amphiphilic and depending on their concentration in a solution can exist as individual molecules or molecular aggregates in the bulk as well as on the interface as adsorbed species. While the adsorption of the surfactant to the interface leads to a reduction in the interfacial tension (both dynamic and equilibrium), their self-association in the bulk minimizes the interaction between the solvent and the lyophobic part of the surfactant molecules. The aggregates of surfactant molecules are typically of well-defined shapes depending on the chemical nature of the surfactant and the solvent, temperature, solution conditions, and so forth. However, this self-association required a minimum concentration of surfactant molecules in the solution. The critical concentration at which the micelles begin to form is called the critical micellar concentration (CMC). Depending on the nature of the lyophilic and lyophobic parts, the surfactant molecules can self-associate in the solution into a variety of structures such as micelles, reverse micelles, vesicles, bilayers,

and so forth. The surface active property and the ability of surfactants to form molecular aggregates is exploited in a range of applications in areas as diverse as detergents, cosmetics, textiles, leather, paints, paper, ore flotation, emulsions, pharmaceuticals, and so forth.[1−5] The CMC is important in all of the industrial processes mentioned above. In these processes, whether it is used in lowering of the interfacial tension required for emulsification, stabilization of particulate dispersions, promoting foam stability, or as delivery vehicles as molecular aggregates, it is typically achieved when the concentration of the surfactant is significantly above the CMC.
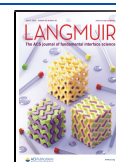
When micelles begin to form, the surfactant solution behaves as a microheterogeneous medium and is often characterized by a discontinuity in the system properties. Therefore, CMC can be determined by noting the change in different physicochemical properties and processes as the concentration of the surfactant is varied across CMC. And hence, CMC has been measured by monitoring surface tension,[6] electrical conductivity,[7] dye solubility,[8,9] pulse radiolysis,[10] light scattering,[11] density,[12,13] viscosity,[13,14] refractive index,[15−17] spectrofluorometry,[18,19] isothermal titration calorimetry,[20,21] ultrasonic absorption,[22] turbidity,[23] pH,[24] and spreading kinetics.[25]

It must be noted that among the methods mentioned above, the CMC detected by measuring the surface tension exploits the change in the concentration of the surfactant molecules adsorbed at the interface, while most of the other methods exploit the measurement of any property associated with the formation of micelles in the bulk. Since the spreading of fluids depends on the interfacial tension, adsorption of surfactant molecules at an interface can also influence the spreading behavior.[26] The spreading process of surfactant laden systems has been extensively studied.[25,27−35] However, most of the studies are carried out when the surfactant is added to the spreading liquid (drops). Moreover, the scope of most of the previous research has been limited to the study of spreading dynamics of surfactant solutions at concentrations either above the CMC or below the CMC.[36−39] As the variation of interfacial tension as a function of surfactant concentration is different above and below the CMC, the spreading behavior is also expected to vary across the CMC, which is the subject of the current investigation.

In this work, we study the spreading behavior of oil drops on aqueous solutions containing different types of surfactants at concentrations varying across the CMC. To investigate the generality of the spreading process, aqueous solutions containing different types of surfactant—nonionic, cationic, and anionic are considered. As the concentration of the surfactant in the aqueous media is varied across the CMC, we observed a distinct change in the maximum area that the oil drops occupied on the surfactant laden interface. Therefore, this change in spreading behavior, quantified by estimating the maximum spreading area can be used as a simple tool to measure the CMC of the surfactant, irrespective of whether the surfactant is ionic or nonionic. Furthermore, the robustness of this method was verified by changing the diameter of the Petri dish, the volume of the oil drop, and the height of the aqueous surfactant solution. This study can also provide insight into the fundamental role of surfactants in the wetting and spreading of fluid−fluid systems.

■ EXPERIMENTAL SECTION

Materials. *n*-Decane, $C_{10}H_{22}$ (with a density of 0.730 g/mL, a viscosity of 0.850 mPa·s, and a vapor pressure of 1.43 mmHg, all measured at 25 °C) procured from Alfa Aesar (99% pure) was used as the oil in all the experiments. The choice of decane is due to the fact that its spreading coefficient on pure water is negative (S = −3.4 mN/m) unlike oils such as hexane, heptane, and silicon oil which have positive spreading coefficients. The oils with positive spreading coefficients spread spontaneously occupying the entire area of the Petri dish even on the surface of pure water and therefore are not suited for our experiments. Prior to use, *n*-decane was passed through a column of aluminum oxide (Al_2O_3, Fisher Scientific, Active) to remove surface active impurities, if any. In this study, we use different surfactants, namely, sodium dodecyl sulfate (SDS) of two different

purities (Merck specialties, 90%) and (Sigma-Aldrich, 99%), cetyltrimethylammonium bromide (CTAB, Sigma-Aldrich, 98%), dioctyl sodium sulfosuccinate (AOT, Sigma-Aldrich, 97%), polysorbate 80 (Tween 80, Merck), and polyethylene glycol *tert*-octylphenyl ether (Triton X-100, Sigma-Aldrich, 98%). The chemical structures of the surfactants used in this study are shown in Figure 1.
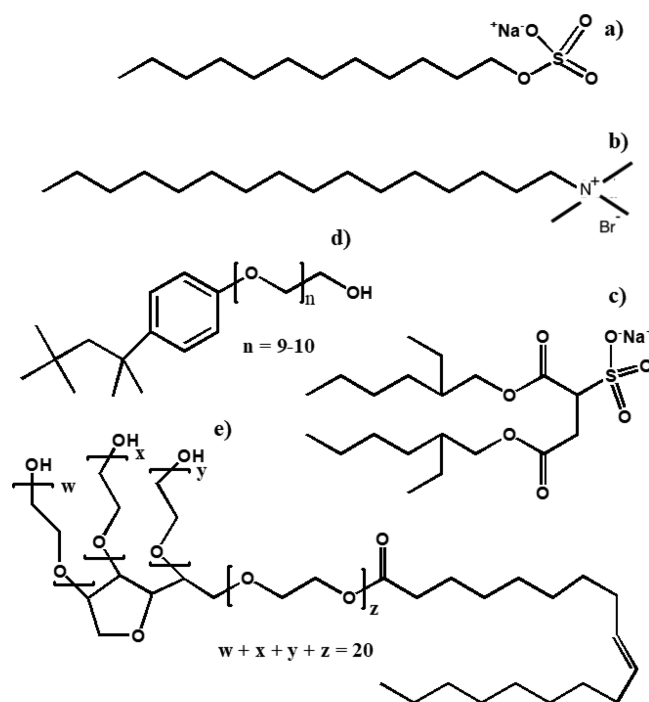
Figure 1. Chemical structure of surfactants used in the spreading experiments: (a) SDS, (b) CTAB, (c) AOT, (d) Triton X-100, and (e) Tween 80.

All the surfactants were used as received without further treatment. The aqueous surfactant solutions were prepared by adding a known quantity of surfactant into ultrapure Milli-Q water (18.2 MΩ·cm, Merck Millipore) of known volume.

Experimental Setup. Figure 2 shows the experimental setup used for spreading experiments. All experiments were carried out in a steel box to avoid the effect of any external disturbance. The oil drop was gently placed on an aqueous solution taken in a Petri dish kept inside the box. A light source mounted at the top of the box was used for visualization of the spreading front. To modulate the intensity of this
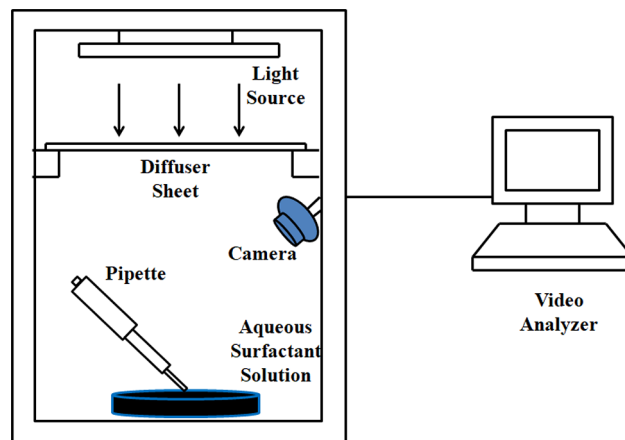
Figure 2. Experimental setup used for studying spreading of oil drops on aqueous surfactant solutions.

Table 1. Details of Surfactants and Their Concentrations Used in Spreading Experiments

Surfactant	Type	Concentration range studied (mM)	Molecular weight (g/mol)	Hydrophilic-lipophlic balance (HLB)
SDS	anionic	0.1−14.0	288.37	40
CTAB	cationic	0.6−1.4	364.45	10
AOT	anionic	1.0−3.4	444.56	32
Triton X-100	nonionic	0.08−0.32	647.00	13.5
Tween 80	nonionic	0.001−0.048	1310.00	15
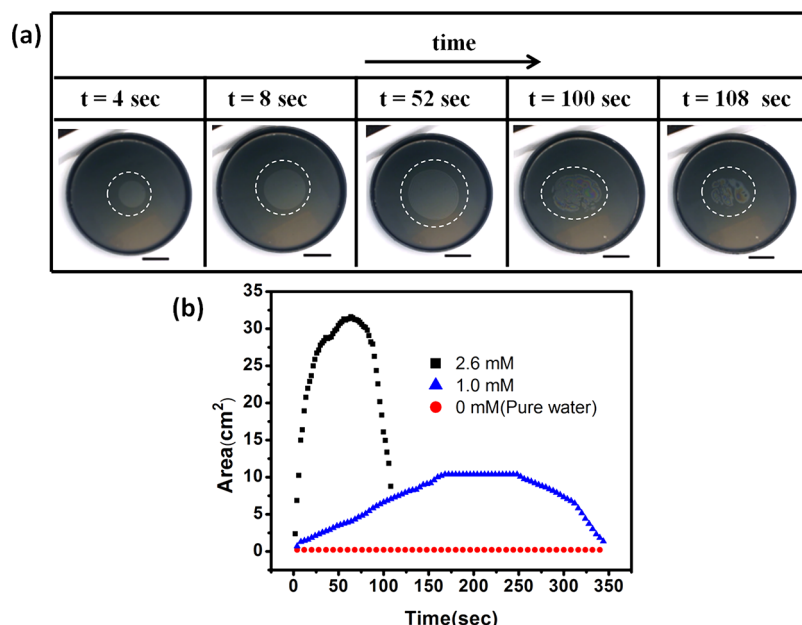
Figure 3. (a) Top view of the oil drop spreading on 2.6 mM aqueous AOT solution as a function of time. A dashed line is drawn around the spreading drop to demarcate the area occupied by oil drop in each frame. The black scale bar in all images represents 3 cm. The experiments are carried out by placing a 5 μL oil drop on the surface of a 4 mm thick pure water and aqueous surfactant solution taken in a 12.6 cm diameter Petri dish. (b) The temporal evolution of the projected area of the oil drop spreading on pure water, 1.0 and 2.6 mM aqueous AOT solutions. While the projected area of the oil drop does not change with time for pure water, it exhibits a maximum for the two solutions.

light source, a diffuser sheet was fixed beneath the light source. An iBall webcam (CHD20.0) placed below the diffuser sheet was used to record the spreading of the oil drop at 30 frames/sec. The images extracted from the video were analyzed and the area of the spreading drop was measured using ImageJ software. The "find edges" tool in ImageJ software which identifies sharp changes in intensity was used to determine the edge of the droplet. The reported values of the projected area have been corrected for the angle of observation by scaling with the dimensions of the Petri dish. This correction can be done since the observation angle affects the projected area of the spreading oil drop and the Petri dish in a similar fashion. The experimental setup was placed on a vibration isolation table to eliminate influence of external vibrations. All spreading experiments were carried out at a temperature of 28 ± 1 °C.

Spreading Experiments. Aqueous surfactant solutions of various concentrations below and above CMC, range shown in Table 1, were prepared to carry out the spreading experiments. In a typical spreading experiment, 50 mL of surfactant solution was transferred to a polystyrene Petri dish of 12.6 cm inner diameter. This leads to a 4 mm deep substrate liquid (i.e., surfactant solution) in the Petri dish.

The outer surface of the transparent Petri dish was coated with an acrylic lacquer black paint, which was essential to improve the contrast and to enable easy visualization of the spreading of the oil drops. The oil drops were spread on the surfactant solution only after a waiting period. This procedure ensured that the concentration of surfactant molecules at the solution−air interface reaches equilibrium. In our spreading experiments that have been reported, the waiting period was fixed at 6 h. A 5 μL drop of decane was delicately placed on the aqueous surfactant solution−air interface using a micropipette
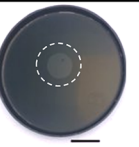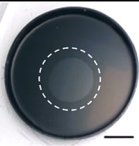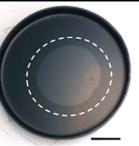
in such a way that it produced minimal disturbance to the bulk of the aqueous surfactant solution.

A liquid spreading on another can form a precursor film surrounding the liquid lens depending on the fluid−fluid−surfactant combination. To check the presence of precursor films, if any, few spreading experiments were carried out with aqueous surfactant solutions on which talc powder was sprinkled a priori. The spreading behaviors of the droplet with and without talc powder were compared.

Each spreading experiment was repeated at least 3 times. To check the robustness of the observations, the spreading experiments were carried out by varying three different parameters such as the Petri dish diameter (12.6, 9.9, and 7.2 cm), oil drop volume (5 and 10 μL), and the depth of the aqueous surfactant solution in the Petri dish (2, 4, and 10 mm). Experiments were performed by changing one parameter at a time while the other two parameters were kept constant.

CMC by Surface Tension Measurement. The interfacial tension between aqueous surfactant solutions and air was measured using a tensiometer (Model-Kruss DSA256E) by the pendant drop method. This method uses image analysis to determine the drop shape and the Young−Laplace equation to find the interfacial tension. Prior to using the surfactant solution samples, the surface tension of the water−air interface was determined and found to be 72 ± 0.3 mN/m. The interfacial tension of alumina treated decane and water was also measured before carrying out spreading experiments and was found to be 51.9 ± 0.2 mN/m, indicating the absence of surface active impurities.

The equilibrium surface tension values when the surface tension reached a constant value with time was determined. The CMC of

Figure 4. The maximum area occupied by the oil drop spreading on aqueous CTAB, AOT, and Tween 80 solutions of different concentrations. The surfactant concentration is indicated on the top of each image. The dashed line around the spreading drop demarcates the area occupied by the oil drop in each frame. The black scale bar in all images represents 3 cm.
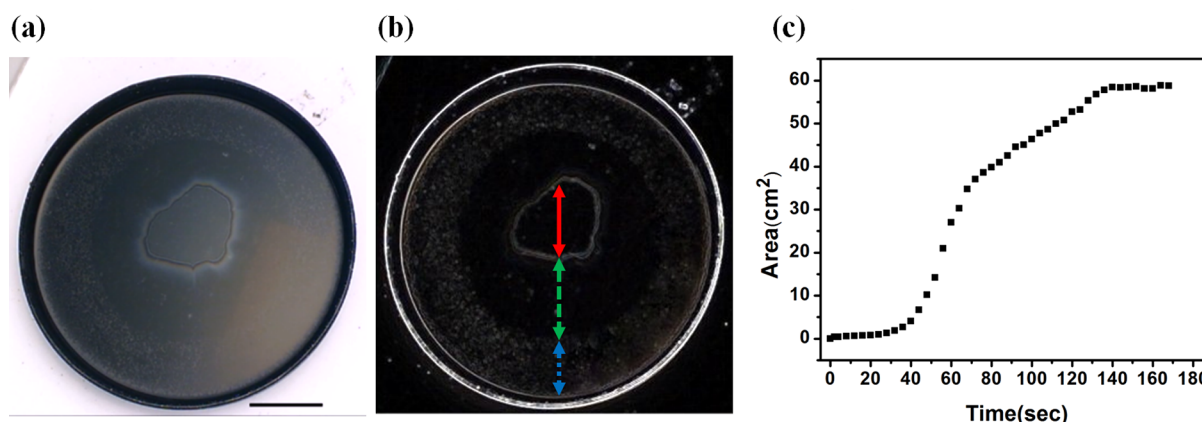
Figure 5. Spreading of an oil drop on 0.12 mM aqueous Triton X-100 solution in which precursor film is observed: (a) Top view of an oil drop at t = 124 s. The scale bar represents 3 cm. (b) The image in (a) processed using ImageJ software to distinguish the main lens (continuous line with double arrow), precursor film (dashed line with double arrow) and the aqueous surfactant solution−air interface containing talc powder (dotted line with double arrow). (c) The variation of total projected area (main lens+precursor film) with time. The acquisition of the data is discontinued after the main lens completely disappeared. Thereafter, the precursor is observed to dissolve into the bulk of the solution.

surfactants was determined by plotting the equilibrium surface tension against the surfactant concentration. The surface tension measurements were carried out at the same temperature (28 ± 1 °C) at which the spreading experiments were performed.

CMC by Conductivity Measurements. The CMC of ionic surfactants were determined by measuring the conductivity of the surfactant solutions using an ECON 700 benchtop conductivity meter with 1 cm^{-1} cell constant. The conductivity meter was calibrated with a KCl solution of known concentration prior to the measurements. All measurements were performed at 28 ± 1 °C. A plot of conductivity versus surfactant concentration showed two distinct linear regimes, with their intersection giving the CMC. The conductivity measurements were repeated 3 times to check the accuracy of the data.

■ RESULTS AND DISCUSSION

Spreading and Dissolution of Oil Drops on Aqueous Surfactant Solutions. An oil drop introduced on the surface of an aqueous surfactant solution spreads to minimize the surface free energy. In our experiments, we consider the spreading of oil drops on aqueous solutions of ionic (CTAB, AOT, SDS) and nonionic (Tween 80, Triton X-100) surfactants. As will be discussed further, the oil drops either form a lens or a film, which may ultimately dissolve into the aqueous phase. This depends on the concentration and type of the surfactant as well as the interfacial tension of the liquids. The ability of the oil drop to spread on the aqueous solutions can be inferred by calculating the spreading coefficient (S), which is defined as follows:
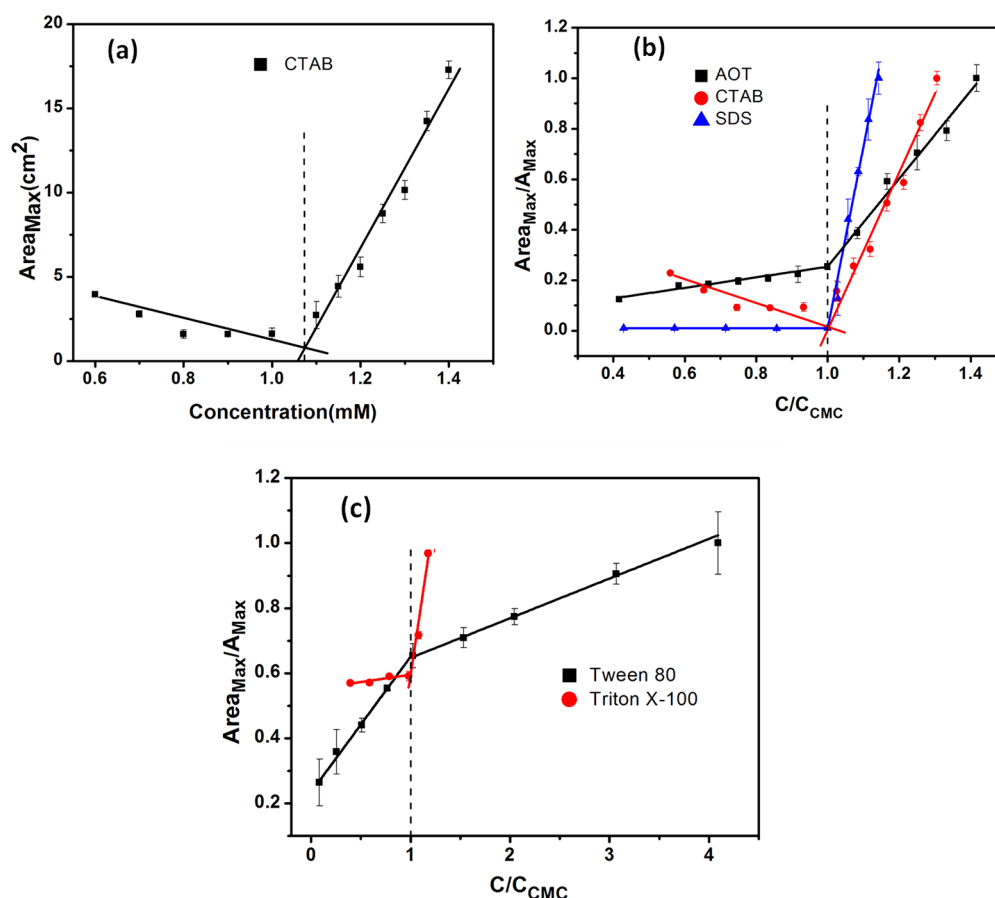
Figure 6. Determination of CMC from spreading experiments: (a) The maximum projected area occupied by oil drops spreading on aqueous CTAB solutions of different concentrations. The variation in the area can be captured by two straight lines of different slopes which intersect at CMC. The straight lines are best fit to the experimental data with a coefficient of regression >0.95. The maximum projected area vs concentration for various (b) ionic and (c) nonionic surfactants. Note that in (b) and (c), the surfactant concentration is normalized with the CMC of respective surfactant and the maximum projected area at a particular concentration ($Area_{max}$) is normalized with the maximum projected corresponding to the highest concentration of the surfactant (A_{max}). The dashed vertical line is drawn at $C/C_{CMC} = 1$. In all these experiments, 5 μL decane drops are placed on an aqueous surfactant solution filled up to a height of 4 mm in a Petri dish of 12.6 cm diameter.

$$S = \gamma_1 - \gamma_2 - \gamma_{12} \qquad (1)$$

where, γ_1 is the interfacial tension between the aqueous solution and air, γ_2 is the interfacial tension between oil and air, and γ_{12} is the interfacial tension between aqueous solution and oil. If $S > 0$, then the oil drop tends to spread over the aqueous solution forming a thin film, and if $S < 0$, the oil drop is expected to form a lens. The spreading coefficient only indicates whether the spreading of one liquid over another is thermodynamically favorable or not, but it does not indicate either the kinetics of spreading or the final state of the oil drop that is placed on the aqueous surfactant solution.

Prior to investigating the spreading of oil drops on a surfactant laden aqueous solution, experiments were performed with decane and water as test fluids without any surfactants. It was observed that oil forms a lens on the surface of the water, in agreement with the literature.[40,41]

We now consider oil drops spreading on aqueous AOT solutions as a typical case to illustrate the spreading behavior in our experiments. Once the oil drop is placed on the surfactant laden interface, there are two processes that occur simultaneously: the spreading of oil drop and its dissolution into the surfactant solution. However, the spreading process that dominates at initial times is expected to lead to an increase in the area that the oil drop occupies at the interface and the

dissolution which is more dominant in the final stages results in a reduction in the area that the oil drop occupies. The kinetics and dissolution of decane drop spreading on aqueous solutions of 2.6 mM AOT concentration is shown in Figure 3(a). The figure shows the top view of the oil drop at various instances of time during the spreading process. Note that the difference in the refractive indices of the fluids involved is small which leads to poor contrast in the images. Therefore, a dashed curve that encloses the oil lens is drawn to guide the eye. The projected area of the oil drop measured as a function of time is plotted in Figure 3(b) for two different AOT concentrations. At the initial stages of spreading, the oil drop forms a lens, and the projected area is small. Further, the projected area increases and reaches a maximum as shown in Figure 3(b).

The oil film ultimately dissolves into the aqueous surfactant solution and therefore, the projected area decreases. This dissolution is due to the emulsification of oil into water stabilized by the surfactants.[42−45] While the increase in the projected area is due to the spreading of the oil drop, the drastic reduction is due to the dissolution process. It must be noted that the rate of the initial increase in the projected area is higher at larger (2.6 mM) AOT concentration compared to the 1.0 mM AOT concentration. Therefore, the maximum occurs at an earlier time when the AOT concentration is higher.
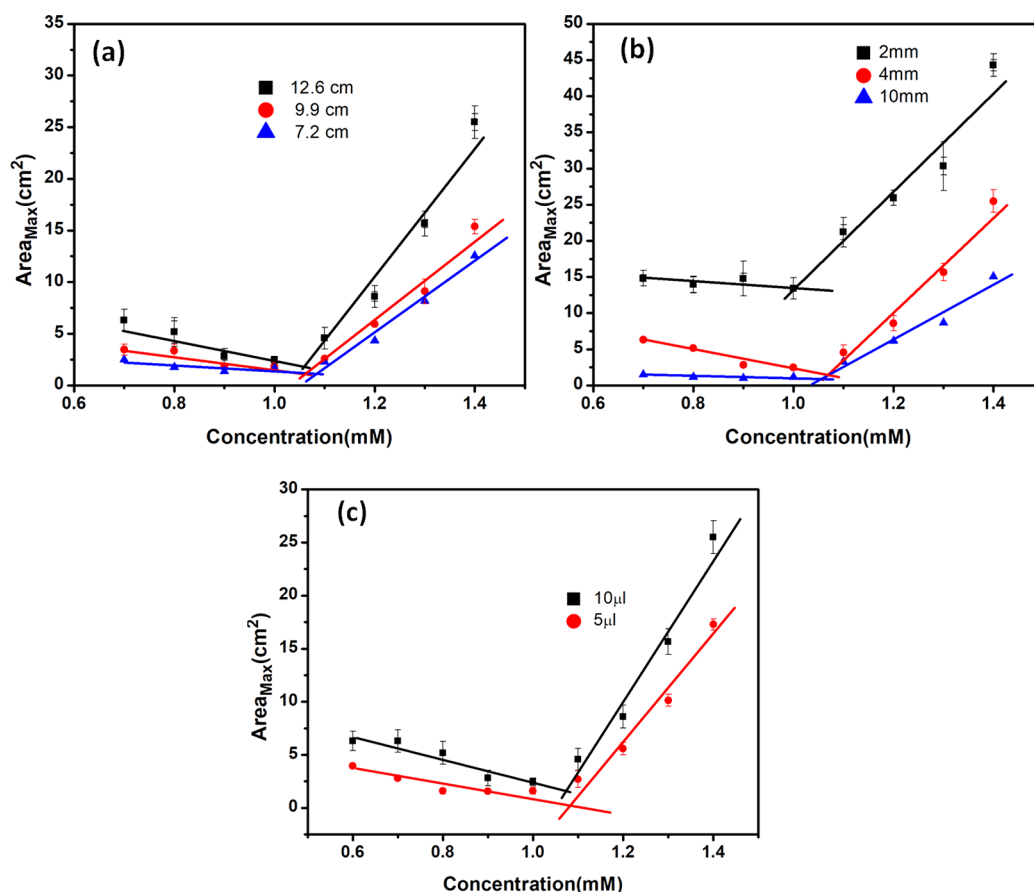
Figure 7. (a)Effect of Petri dish diameter on CMC measurement: The experiments are conducted by placing 10 μL decane drops on aqueous CTAB solutions filled up to a height of 4 mm. (b) Effect of substrate liquid height on CMC measurement: The experiments are conducted by placing 10 μL decane drops on aqueous CTAB solutions taken in a Petri dish of 12.6 cm diameter. The CMC determined using a 2 mm substrate liquid height is slightly lower probably due to the effect of solid surface underneath the surfactant solution. (c) Effect of oil drop volume on CMC measurement: The experiments are conducted by placing 5 μL and 10 μL decane drops on aqueous CTAB solutions taken in a Petri dish of 12.6 cm diameter filled up to a height of 4 mm. The straight lines in the plots are best fit to the experimental data with a coefficient of regression >0.95.
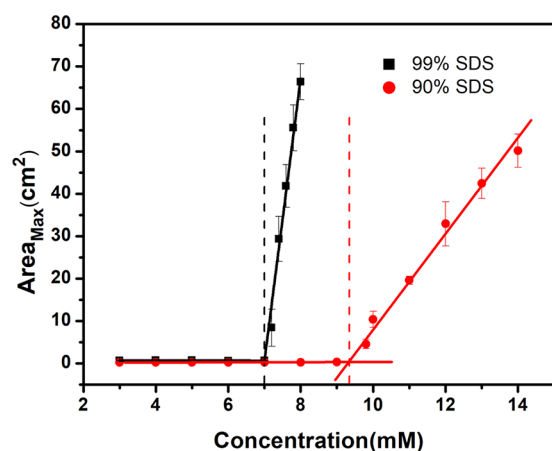
Figure 8. Determination of CMC of surfactants of differing purity from spreading experiments. The maximum projected area occupied by oil drops spreading on aqueous SDS solutions of 99% and 90% purity is plotted as a function of concentration. The variation in the area captured by two straight lines of different slopes intersect at significantly different concentrations indicating the influence of surfactant purity on CMC.

Moreover, the magnitude of the maximum projected area is also higher. Therefore, a progressive shift in the magnitude of

the maximum projected area occurs as the concentration of surfactant in the aqueous solution increases, a feature which will be discussed further.

The existence of a maximum in the projected area of the drop spreading on aqueous solutions is not restricted to the case described above, but occurs irrespective of the surfactant concentrations or the type of surfactant used. We believe that this unique state, i.e., the state corresponding to the maximum projected area points to the generality of the spreading dissolution process in these systems and can therefore be exploited further to investigate the interplay of the dynamics and partitioning of the surfactants in the bulk and at the interface. Figure 4 shows this maximum in the projected area of the oil drop on the surface of the solutions of different types of surfactant and at various concentrations. Comparison of the spreading patterns in each image shown in Figure 4 points to the difference in the shape and area occupied by the oil lens when the concentration of the surfactant in the aqueous solution is varied. Clearly, the maximum projected area changes with the increase in the concentration of the surfactant in the aqueous phase irrespective of the types of surfactant used, i.e., cationic (CTAB), anionic (AOT), or nonionic (Tween 80).

The thermodynamical quantity, spreading coefficient, defined by eq 1 alone does not explain the above observations,

Table 2. Comparison of the CMC Determined by Drop Spreading Method with Conventional Techniques and Also Reported Values from the Literature at 25 °C

Surfactant	CMC by image analysis(mM)	CMC by surface tension(mM)	CMC by Conductivity(mM)	CMC from literature
SDS (99%)	7.00	7.89	8.64	7.4−8.7[49−52]
CTAB	1.07	1.00	0.95	0.93−1.00[53−56]
AOT	2.40	2.51	no inflection	2.50−2.66[6,57−59]
Triton X-100	0.20	0.25		0.15−0.28[60−64]
Tween 80	0.011	0.010		0.012−0.018[65−67]
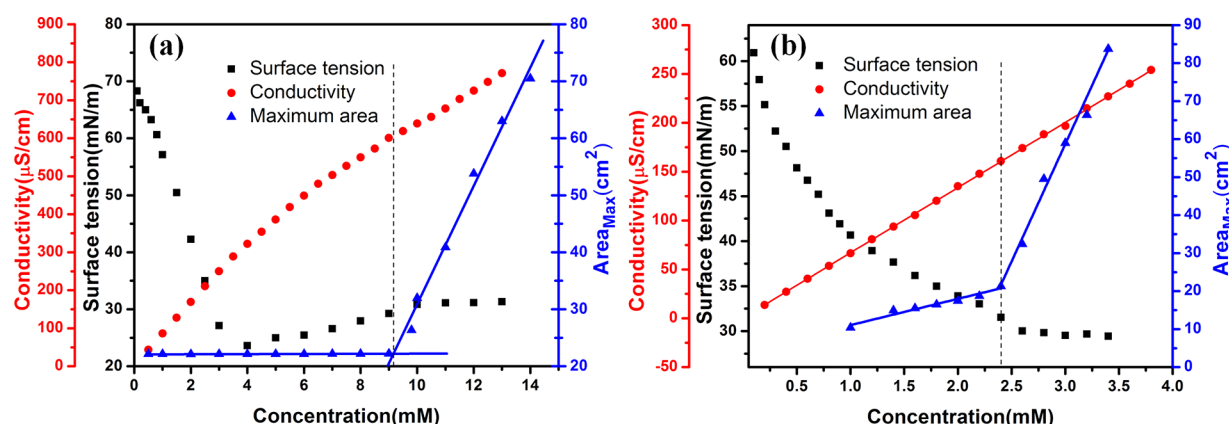
Figure 9. A comparison of the CMC determination techniques by measurement of surface tension, ionic conductivity, and the maximum projected area during spreading for (a) 90% pure SDS and (b) AOT.

such as the occurrence of a maximum in the projected area of the oil lens and its dependence on the surfactant concentration for two reasons: (1) The spreading coefficient is calculated based on the equilibrium interfacial tensions for the aqueous surfactant-oil-air system, the measurement of which requires an equilibration time typically on the order of 5 to 10 min. Alternatively, the occurrence of the maximum projected area takes less time (a few minutes or less). Therefore, clearly the maximum projected area is a characteristic feature associated with the dynamics of the spreading process. (2) When an oil drop is placed on the surface of an aqueous surfactant solution, the drop spreads, increasing its contact with the substrate solution. At the same time, the oil drop also dissolves into the solution. These two processes which occur simultaneously lead to the occurrence of a maximum in the projected area of the oil drop. As the concentration of the surfactant is varied, both the spreading and dissolution processes are affected and therefore, the maximum projected area is not determined solely by spreading, i.e., the equilibrium spreading coefficient.

Spreading and Dissolution in the Presence of Precursor Films. The formation of precursor films in the case of liquid drops spreading on surfaces is well studied.[46,47] The characteristic feature of the precursor film is that it extends beyond the apparent three phase contact line and is difficult to visualize with the naked eye as its thickness varies from the molecular to the submicron level.[48] The precursor film advances faster than the spreading of the macroscopically observable part of the liquid lens. In this section, we consider the case of the spreading of oil drops on the surface of aqueous SDS and Triton X-100 solutions where the precursor film formation is evident. In the experiments described below, the visualization of the spreading process and the measurement of the projected area was carried out by sprinkling talc powder particles on the surface of the aqueous solution before the drop is introduced. The surface tension of the water−air (and

water−decane) interface in the presence of talc powder was found to be same as that of the pristine water−air (and water−decane) interface indicating the absence of any surface active species in the powder and hence is not expected to influence the spreading of oil drops.

The precursor film if present pushes the talc powder particles away before the main lens does. Figure 5 shows the top view of an oil drop spreading on Triton X-100 laden aqueous solution. Three regions can be identified in Figure 5(a), which are more distinctly visible in the processed image obtained after edge detection as shown in Figure 5(b). The central region marked by a solid line with double headed arrow is the main lens, surrounded by the region of the precursor film, marked by a dashed line with a double-headed arrow. Beyond the precursor film until the edge of the Petri dish is the aqueous solution−air interface where the talc powder particles pushed away by the spreading precursor film front are concentrated. This region is marked by a dotted line with double-headed arrow.

In the presence of the precursor films, in the initial stages of spreading, the total projected area (of the main lens and the precursor film) is small, which further increases rapidly with time, reaches a maximum. This observation is similar to the behavior shown in Figure 3(b). However, we did not observe the dissolution of the precursor film into the aqueous solution and the total projected area remains unchanged during the experimental time scale. The time variation of the total projected area for the spreading of oil drops on Triton X-100 laden aqueous solution interface is shown in Figure 5(c). We have observed that this behavior is general as tested for the spreading of oil drops on aqueous solutions at various concentrations of SDS (anionic) and Triton-X 100 (nonionic). Therefore, irrespective of the concentration, surfactant type, and presence of precursor film, there exists a maximum in the

total projected area when the oil drops spread and dissolve on aqueous surfactant solutions.

CMC from Spreading Experiments. In this section, we demonstrate that the change in the maximum projected area of the oil drop with change in concentration of the surfactant in the aqueous phase can be exploited to determine the CMC of the surfactants in solution. Figure 6(a) shows the variation in the maximum projected area, $Area_{max}$, as the concentration of CTAB in the aqueous phase is systematically increased. It must be noted that this variation in $Area_{max}$ can be captured by two straight lines of different slopes.

Interestingly, these two straight lines intersect at a concentration that coincides with the CMC of CTAB. When the concentration is lower than CMC, the slope of the straight line is much smaller indicating weak dependence of maximum projected area with concentration. However, when the concentration is higher than the CMC, the projected area increases drastically with the increase in surfactant concentration. Therefore, from the data presented in Figure 6(a), we can conclude that the maximum projected area of the drop introduced on the surface of aqueous surfactant solutions shows a distinct change at CMC, a feature that can be exploited to determine the CMC of the surfactant solutions.

We now generalize this methodology to determine the CMC of various types of surfactants. Figure 6(b) and (c) shows the maximum projected area of the oil drop with change in concentration of cationic (CTAB), anionic (AOT, SDS) and nonionic (Tween 80, Triton X-100) surfactants in the aqueous phase. Since the CMC of these surfactants vary by about 1 order of magnitude, we normalize the concentration of each surfactant in the solution with CMC of the respective surfactant. We have also normalized the maximum projected area, $Area_{max}$, with the area corresponding to the highest surfactant concentration considered in our experiments, A_{max}. Interestingly, the two straight lines intersect at $C/C_{CMC} = 1$, where C is the concentration of the surfactant in the aqueous solution with the CMC represented by C_{CMC}. Note that the slopes of the straight lines below and above CMC depend on the type of surfactant in the aqueous solution possibly due to complex interplay of fluid dynamics resulting from both inertial and Marangoni effects, adsorption and desorption of surfactant molecules to the interface created during spreading, and the three phase contact line dynamics. Although there is no specific trend in the slopes, irrespective of the surfactant type, the straight lines always intersect at the CMC.

Robustness of the Proposed Method for CMC Determination. In order to check the robustness of the proposed strategy, experiments were carried out by (i) changing the diameter of the Petri dish in which the surfactant solution is taken (ii) changing the height of the surfactant solution in the Petri dish (iii) varying the volume of the oil drop used. The results corresponding to the variation of each of these parameters are shown in Figure 7. Remarkably, for all the experimentally variable parameters, the plots show a similar trend with the variation of maximum projected area as a function of surfactant concentration being represented by two straight lines of different slopes intersecting at CMC. From the data shown in Figure 7, it is clear that, while the geometrical parameters (the substrate liquid height, the diameter of the Petri dish, and the drop volume) influence the slopes of the fitted straight lines below and above CMC, the point of intersection of the straight lines and the CMC determined are not influenced by these finite size effects. The dependence of

the slopes on the geometrical parameters can be attributed to the complex interplay of (i) spreading driven by interfacial tensions, (ii) Marangoni stress driven flow arising from the inhomogeneous distribution of surfactant on the interface, (iii) dynamic exchange of surfactant molecules between the bulk and the interface, and (iv) the dissolution of the oil film into the bulk.

However, it must be noted that the variation of the maximum projected area with respect to the concentration below the CMC deviates slightly from the linear behavior for the case of 5 μL drops compared to a better linear dependence for the case of 10 μL drops as shown in Figure 7c. Therefore, it is suggested to use larger volume drops in the spreading experiments for the unambiguous determination of CMC. For the drop volumes considered here, the Bond number is less than 1. Therefore, the weight of the drop and the associated interface deformation may not be relevant in our experiments. Although the spreading experiments reported in this work have a waiting period of 6 h, the CMC determined is the same even with the 1 h waiting period.

Furthermore, we show that this method is also suited to measure the CMC of systems of surfactants of different purity. Figure 8 shows the maximum total projected area of the oil drop plotted against the concentration of surfactant in the aqueous solution for 90% and 99% pure SDS. The CMC determined from the intersection of the straight lines are 7 mM and 9.18 mM, respectively, for 99% and 90% pure SDS. Clearly, the CMC of the surfactants of different purity are significantly different, with the CMC being lower for the surfactant of higher purity. This is probably due to the presence of the surface active impurity, lauryl alcohol in 90% pure SDS, a trend that has been observed in mixed surfactant systems.[7]

Comparison with Other CMC Measurement Techniques. The data presented in Table 2 show a comparison between the CMC determined by the spreading method presented in this article with those obtained by the other measurement techniques that are commonly used. CMC measured via surface tension method (for all the surfactants used in this work) and conductivity (SDS and CTAB) as well as those reported in literature are in good agreement with the CMC determined by the spreading method.

Advantages of the Proposed Technique over Other Methods. In certain cases, existing techniques are not suited to measure the CMC, two examples of which are discussed in this section. Figure 9(a) and (b) shows plots of conductivity, surface tension, and maximum projected area as a function of surfactant concentration for 90% pure SDS and AOT, respectively. Typically, the surface tension of fluid-air remains unchanged when the surfactant concentration is extremely low, decreases monotonically with a further increase in concentration, and then reaches a plateau beyond the CMC. However, as shown in Figure 9(a), the surface tension as a function of surfactant concentration for 90% SDS shows a decrease followed by an increase before reaching the plateau. This nonmonotonic behavior is caused by the surface-active impurity lauryl alcohol present in SDS. Therefore, the surface tension measurements make the CMC determination in this case not feasible because of the slope change occurring at multiple concentrations.[7]

The conductivity measurements also suffer from similar issues. The conductivity vs surfactant concentration for 90% pure SDS shows multiple points where slope changes occur

and there is no distinct change in the slope in the case of AOT.[68] Therefore, in such cases, the CMC determination from conductivity measurements is either not possible or ambiguous.

In contrast, the projected area of the oil lens plotted against the surfactant concentration obtained through the proposed method shows a sharp change in the slope that is distinct and therefore enables the unambiguous determination of the CMC. Moreover, as we demonstrated in the previous section, this technique can be used to determine the CMC irrespective of the surfactant type, i.e., cationic, anionic, or nonionic.

CONCLUSIONS

In this work, the spreading of oil drops on aqueous solutions of various types of surfactants is investigated by video microscopy and quantitative image analysis. The experiments conducted by spreading oil drops on aqueous solutions containing surfactants over a large concentration range varying across the CMC show the occurrence of a maximum in the projected area of the oil lens. This unique behavior is observed irrespective of the type and concentration of the surfactant. Moreover, the variation of the maximum in the projected area with respect to the concentration is strikingly different when the concentration is lower or higher than the CMC. We show that this distinct change provides a quantitative measure of the CMC of the surfactant in solution. Interestingly, this behavior is universal and hence this technique can be used to determine the CMC irrespective of the surfactant purity, type (cationic, anionic, or nonionic), and other system variables.

AUTHOR INFORMATION

Corresponding Authors

    Sumesh P. Thampi − *Polymer Engineering and Colloid Sciences Lab, Department of Chemical Engineering, Indian Institute of Technology Madras, Chennai 600036, India*; Email: sumesh@iitm.ac.in

    Madivala G. Basavaraj − *Polymer Engineering and Colloid Sciences Lab, Department of Chemical Engineering, Indian Institute of Technology Madras, Chennai 600036, India*; orcid.org/0000-0002-8275-5671; Email: basa@iitm.ac.in

Authors

    Swaraj Deodhar − *Polymer Engineering and Colloid Sciences Lab, Department of Chemical Engineering, Indian Institute of Technology Madras, Chennai 600036, India*

    Pankaj Rohilla − *Polymer Engineering and Colloid Sciences Lab, Department of Chemical Engineering, Indian Institute of Technology Madras, Chennai 600036, India*; orcid.org/0000-0002-1918-9902

    M Manivannan − *Department of Applied Mechanics, Indian Institute of Technology Madras, Chennai 600036, India*

Complete contact information is available at:
https://pubs.acs.org/10.1021/acs.langmuir.0c00908

Notes

The authors declare no competing financial interest.

ACKNOWLEDGMENTS

REFERENCES

(1) Rosen, M. J.; Kunjappu, J. T. et al. *Surfactants and Interfacial Phenomena*; Wiley Online Library, 2004; Vol. 82.

(2) Myers, D. *Surfactant Science and Technology*; Wiley Online Library, 2006.

(3) Karsa, D. R. *Industrial Applications of Surfactants IV*; Elsevier, 1999.

(4) Kronberg, B.; Lindman, B. *Surfactants and Polymers in Aqueous Solution*; John Wiley & Sons Ltd.: Chichester, 2003.

(5) Schramm, L. L.; Stasiuk, E. N.; Marangoni, D. G. 2 Surfactants and their applications. *Annu. Rep. Prog. Chem., Sect. C: Phys. Chem.* **2003**, *99*, 3−48.

(6) Mahajan, R. K.; Sharma, R. Analysis of interfacial and micellar behavior of sodium dioctyl sulphosuccinate salt (AOT) with zwitterionic surfactants in aqueous media. *J. Colloid Interface Sci.* **2011**, *363*, 275−283.

(7) Lin, S.-Y.; Lin, Y.-Y.; Chen, E.-M.; Hsu, C.-T.; Kwan, C.-C. A study of the equilibrium surface tension and the critical micelle concentration of mixed surfactant solutions. *Langmuir* **1999**, *15*, 4370−4376.

(8) Ross, S.; Olivier, J. A new method for the determination of critical micelle concentrations of un-ionized associations colloids in aqueous or in non-aqueous solution. *J. Phys. Chem.* **1959**, *63*, 1671−1674.

(9) Mukerjee, P.; Mysels, K. J. A Re-evaluation of the Spectral Change Method of Determining Critical Micelle Concentration1. *J. Am. Chem. Soc.* **1955**, *77*, 2937−2943.

(10) Perkowski, J.; Mayer, J.; Ledakowicz, S. Determination of critical micelle concentration of non-ionic surfactants using kinetic approach. *Colloids Surf., A* **1995**, *101*, 103−106.

(11) Topel, O.; Cakır, B. A.; Budama, L.; Hoda, N. Determination of critical micelle concentration of polybutadiene-block-poly (ethyleneoxide) diblock copolymer by fluorescence spectroscopy and dynamic light scattering. *J. Mol. Liq.* **2013**, *177*, 40−43.

(12) Bielawska, M.; Chodzińska, A.; Jańczuk, B.; Zdziennicka, A. Determination of CTAB CMC in mixed water+ short-chain alcohol solvent by surface tension, conductivity, density and viscosity measurements. *Colloids Surf., A* **2013**, *424*, 81−88.

(13) Kodama, M.; Miura, M. The second CMC of the aqueous solution of sodium dodecyl sulfate. II. Viscosity and density. *Bull. Chem. Soc. Jpn.* **1972**, *45*, 2265−2269.

(14) Mitsionis, A. I.; Vaimakis, T. C. Estimation of AOT and SDS CMC in a methanol using conductometry, viscometry and pyrene fluorescence spectroscopy methods. *Chem. Phys. Lett.* **2012**, *547*, 110−113.

(15) Ekwall, P.; Mandell, L.; Solyom, P. The aqueous cetyl trimethylammonium bromide solutions. *J. Colloid Interface Sci.* **1971**, *35*, 519−528.

(16) Klevens, H. Critical micelle concentrations as determined by refraction. *J. Phys. Colloid Chem.* **1948**, *52*, 130−148.

(17) Tan, C. H.; Huang, Z. J.; Huang, X. G. Rapid determination of surfactant critical micelle concentration in aqueous solutions using fiber-optic refractive index sensing. *Anal. Biochem.* **2010**, *401*, 144−147.

(18) Kalyanasundaram, K.; Thomas, J. Environmental effects on vibronic band intensities in pyrene monomer fluorescence and their application in studies of micellar systems. *J. Am. Chem. Soc.* **1977**, *99*, 2039−2044.

(19) Aguiar, J.; Carpena, P.; Molina-Bolívar, J.; Ruiz, C. C. On the determination of the critical micelle concentration by the pyrene 1:3 ratio method. *J. Colloid Interface Sci.* **2003**, *258*, 116−122.

(20) Li, X.; Wettig, S. D.; Verrall, R. E. Isothermal titration calorimetry and dynamic light scattering studies of interactions between gemini surfactants of different structure and Pluronic block copolymers. *J. Colloid Interface Sci.* **2005**, *282*, 466−477.

(21) Heerklotz, H.; Seelig, J. Titration calorimetry of surfactant−membrane partitioning and membrane solubilization. *Biochim. Biophys. Acta, Biomembr.* **2000**, *1508*, 69−85.

(22) Frindi, M.; Michels, B.; Levy, H.; Zana, R. Alkanediyl-. alpha.,. omega.-bis (dimethylalkylammonium bromide) Surfactants. 4. Ultrasonic absorption studies of amphiphile exchange between micelles and bulk phase in aqueous micellar solution. *Langmuir* **1994**, *10*, 1140−1145.

(23) Kushner, L. M.; Hubbard, W. D.; Parker, R. A. Turbidity and viscosity measurements on some cationic detergents in water and in sodium chloride solutions. *J. Res. Natl. Bur. Stand.* **1957**, *59*, 113

(24) Chiu, Y.-C.; Yu, K.-M. Simultaneous determination of micellar dissociation concentration and critical micellar concentration of bile salts by pH measurements. *J. Dispersion Sci. Technol.* **1992**, *13*, 587−609.

(25) Roché, M.; Li, Z.; Griffiths, I. M.; Le Roux, S.; Cantat, I.; Saint-Jalmes, A.; Stone, H. A. Marangoni flow of soluble amphiphiles. *Phys. Rev. Lett.* **2014**, *112*, 208302.

(26) Harkins, W. D.; Feldman, A. Films. The spreading of liquids and the spreading coefficient. *J. Am. Chem. Soc.* **1922**, *44*, 2665−2685.

(27) Svitova, T. F.; Hill, R. M.; Radke, C. J. Spreading of aqueous dimethyldidodecylammonium bromide surfactant droplets over liquid hydrocarbon substrates. *Langmuir* **1999**, *15*, 7392−7402.

(28) Stoebe, T.; Lin, Z.; Hill, R. M.; Ward, M. D.; Davis, H. T. Superspreading of aqueous films containing trisiloxane surfactant on mineral oil. *Langmuir* **1997**, *13*, 7282−7286.

(29) Pimienta, V.; Brost, M.; Kovalchuk, N.; Bresch, S.; Steinbock, O. Complex shapes and dynamics of dissolving drops of dichloromethane. *Angew. Chem., Int. Ed.* **2011**, *50*, 10728−10731.

(30) Wodlei, F.; Sebilleau, J.; Magnaudet, J.; Pimienta, V. Marangoni-driven flower-like patterning of an evaporating drop spreading on a liquid substrate. *Nat. Commun.* **2018**, *9*, 820.

(31) Wang, X.; Bonaccurso, E.; Venzmer, J.; Garoff, S. Deposition of drops containing surfactants on liquid pools: Movement of the contact line, Marangoni ridge, capillary waves and interfacial particles. *Colloids Surf., A* **2015**, *486*, 53−59.

(32) Fallest, D. W.; Lichtenberger, A. M.; Fox, C. J.; Daniels, K. E. Fluorescent visualization of a spreading surfactant. *New J. Phys.* **2010**, *12*, 073029.

(33) Afsar-Siddiqui, A. B.; Luckham, P. F.; Matar, O. K. Unstable spreading of aqueous anionic surfactant solutions on liquid films. 2. Highly soluble surfactant. *Langmuir* **2003**, *19*, 703−708.

(34) Sinz, D. K.; Hanyak, M.; Darhuber, A. A. Immiscible surfactant droplets on thin liquid films: Spreading dynamics, subphase expulsion and oscillatory instabilities. *J. Colloid Interface Sci.* **2011**, *364*, 519−529.

(35) Starov, V. M.; de Ryck, A.; Velarde, M. G. On the spreading of an insoluble surfactant over a thin viscous liquid layer. *J. Colloid Interface Sci.* **1997**, *190*, 104−113.

(36) Joos, P.; Van Hunsel, J. Spreading of aqueous surfactant solutions on organic liquids. *J. Colloid Interface Sci.* **1985**, *106*, 161−167.

(37) Berg, S. Marangoni-driven spreading along liquid-liquid interfaces. *Phys. Fluids* **2009**, *21*, 032105.

(38) Cheng, Y.; Ye, X.; Ma, H. R. Solidlike spreading of a liquid/liquid system. *Appl. Phys. Lett.* **2006**, *89*, 47−50.

(39) Bergeron, V.; Langevin, D. Monolayer spreading of polydimethylsiloxane oil on surfactant solutions. *Phys. Rev. Lett.* **1996**, *76*, 3152.

(40) Shafrin, E. G.; Zisman, W. A. Critical surface tension for spreading on a liquid substrate. *J. Phys. Chem.* **1967**, *71*, 1309−1316.

(41) Kunieda, M.; Liang, Y.; Fukunaka, Y.; Matsuoka, T.; Takamura, K.; Loahardjo, N.; Winoto, W.; Morrow, N. R. Spreading of multicomponent oils on water. *Energy Fuels* **2012**, *26*, 2736−2741.

(42) Binks, B. Emulsion type below and above the CMC in AOT microemulsion systems. *Colloids Surf., A* **1993**, *71*, 167−172.

(43) Katepalli, H.; Bose, A. Response of surfactant stabilized oil-in-water emulsions to the addition of particles in an aqueous suspension. *Langmuir* **2014**, *30*, 12736−12742.

(44) Henry, J. V.; Fryer, P. J.; Frith, W. J.; Norton, I. T. Emulsification mechanism and storage instabilities of hydrocarbon-in-water sub-micron emulsions stabilised with Tweens (20 and 80), Brij 96v and sucrose monoesters. *J. Colloid Interface Sci.* **2009**, *338*, 201−206.

(45) Soma, J.; Papadopoulos, K. D. Ostwald ripening in sodium dodecyl sulfate-stabilized decane-in-water emulsions. *J. Colloid Interface Sci.* **1996**, *181*, 225−231.

(46) Leger, L.; Erman, M.; Guinet-Picard, A.; Ausserre, D.; Strazielle, C. Precursor film profiles of spreading liquid drops. *Phys. Rev. Lett.* **1988**, *60*, 2390.

(47) Popescu, M. N.; Oshanin, G.; Dietrich, S.; Cazabat, A. Precursor films in wetting phenomena. *J. Phys.: Condens. Matter* **2012**, *24*, 243102.

(48) Weng, Y.-H.; Wu, C.-J.; Tsao, H.-K.; Sheng, Y.-J. Spreading dynamics of a precursor film of nanodrops on total wetting surfaces. *Phys. Chem. Chem. Phys.* **2017**, *19*, 27786−27794.

(49) Miyamoto, S. The effect of metallic ions on surface chemical phenomena. IV. Surface tension measurement on aqueous solutions of metal dodecyl sulfates. *Bull. Chem. Soc. Jpn.* **1960**, *33*, 375−379.

(50) Schick, M. Effect of temperature on the critical micelle concentration of nonionic detergents. thermodynamics of micelle formation1. *J. Phys. Chem.* **1963**, *67*, 1796−1799.

(51) Rehfeld, S. J. Adsorption of sodium dodecyl sulfate at various hydrocarbon-water interfaces. *J. Phys. Chem.* **1967**, *71*, 738−745.

(52) Woolfrey, S.; Banzon, G.; Groves, M. The effect of sodium chloride on the dynamic surface tension of sodium dodecyl sulfate solutions. *J. Colloid Interface Sci.* **1986**, *112*, 583−587.

(53) Das, C.; Das, B. Thermodynamic and interfacial adsorption studies on the micellar solutions of alkyltrimethylammonium bromides in ethylene glycol (1)+ water (2) mixed solvent media. *J. Chem. Eng. Data* **2009**, *54*, 559−565.

(54) Okuda, H.; Imae, T.; Ikeda, S. The adsorption of cetyltrimethylammonium bromide on aqueous surfaces of sodium bromide solutions. *Colloids Surf.* **1987**, *27*, 187−200.

(55) Kile, D. E.; Chiou, C. T. Water solubility enhancements of DDT and trichlorobenzene by some surfactants below and above the critical micelle concentration. *Environ. Sci. Technol.* **1989**, *23*, 832−838.

(56) Zhu, Y.; Xu, G.; Xin, X.; Zhang, H.; Shi, X. Surface tension and dilational viscoelasticity of water in the presence of surfactants tyloxapol and Triton X-100 with cetyl trimethylammonium bromide at 25 C. *J. Chem. Eng. Data* **2009**, *54*, 989−995.

(57) Li, Z.; Lu, J.; Thomas, R. Neutron reflectivity studies of the adsorption of aerosol-OT at the air/water interface: the surface excess. *Langmuir* **1997**, *13*, 3681−3685.

(58) Chakraborty, A.; Chakraborty, S.; Saha, S. K. Temperature dependant micellization of AOT in aqueous medium: effect of the nature of counterions. *J. Dispersion Sci. Technol.* **2007**, *28*, 984−989.

(59) Umlong, I.; Ismail, K. Micellization of AOT in aqueous sodium chloride, sodium acetate, sodium propionate, and sodium butyrate media: A case of two different concentration regions of counterion binding. *J. Colloid Interface Sci.* **2005**, *291*, 529−536.

(60) Makievski, A.; Fainerman, V.; Joos, P. Dynamic surface tension of micellar Triton X-100 solutions by the maximum-bubble-pressure method. *J. Colloid Interface Sci.* **1994**, *166*, 6−13.

(61) Rharbi, Y.; Kitaev, V.; Winnik, M. A.; Hahn, K. G. Characterizing aqueous micellar Triton X-100 solutions of a fluorescent model triglyceride. *Langmuir* **1999**, *15*, 2259−2266.

(62) Ruiz, C. C.; Molina-Bolivar, J.; Aguiar, J.; MacIsaac, G.; Moroze, S.; Palepu, R. Thermodynamic and structural studies of Triton X-100 micelles in ethylene glycol- water mixed solvents. *Langmuir* **2001**, *17*, 6831−6840.

(63) Nemethy, G.; Ray, A. Micelle formation by nonionic detergents in water-ethylene glycol mixtures. *J. Phys. Chem.* **1971**, *75*, 809−815.

(64) Göbel, J.; Joppien, G. Dynamic Interfacial Tensions of Aqueous Triton X-100 Solutions in Contact with Air, Cyclohexane, n-Heptane, andn-Hexadecane. *J. Colloid Interface Sci.* **1997**, *191*, 30−37.

(65) Samanta, S.; Ghosh, P. Coalescence of air bubbles in aqueous solutions of alcohols and nonionic surfactants. *Chem. Eng. Sci.* **2011**, *66*, 4824−4837.

(66) Ruiz-Peña, M.; Oropesa-Nuñez, R.; Pons, T.; Louro, S. R. W.; Pérez-Gramatges, A. Physico-chemical studies of molecular interactions between non-ionic surfactants and bovine serum albumin. *Colloids Surf., B* **2010**, *75*, 282−289.

(67) Patist, A.; Bhagwat, S.; Penfield, K.; Aikens, P.; Shah, D. On the measurement of critical micelle concentrations of pure and technical-grade nonionic surfactants. *J. Surfactants Deterg.* **2000**, *3* (1), 53−58, DOI: 10.1007/s11743-000-0113-4.

(68) Das, D.; Dey, J.; Chandra, A.; Thapa, U.; Ismail, K. Aggregation behavior of sodium dioctylsulfosuccinate in aqueous ethylene glycol medium. A case of hydrogen bonding between surfactant and solvent and its manifestation in the surface tension isotherm. *Langmuir* **2012**, *28*, 15762−15769.